


Article

Behavior of TiO₂ and CeO₂ Nanoparticles and Polystyrene Nanoplastics in Bottled Mineral, Drinking and Lake Geneva Waters. Impact of Water Hardness and Natural Organic Matter on Nanoparticle Surface Properties and Aggregation

Lina Ramirez ¹, Stephan Ramseier Gentile ², Stéphane Zimmermann ² and Serge Stoll ^{1,*} 

¹ Université de Genève, Institute F.A. Forel, Physico-chimie de l'environnement, Uni Carl Vogt, 66 Bd Carl-Vogt, 1211 Genève 4, Switzerland; Lina.RamirezArenas@unige.ch

² SIG, Industrial Boards of Geneva 2 Ch. du Château-Bloch, Le Lignon, 1211 Genève-2, Switzerland; stephan.ramseier@sig-ge.ch (S.R.G.); stephane.zimmermann@sig-ge.ch (S.Z.)

* Correspondence: serge.stoll@unige.ch; Tel.: +41223790333

Received: 28 February 2019; Accepted: 2 April 2019; Published: 6 April 2019



Abstract: Intensive use of engineered nanoparticles (NPs) in daily products ineluctably results in their release into aquatic systems and consequently into drinking water resources. Therefore, understanding NPs behavior in various waters from naturel to mineral waters is crucial for risk assessment evaluation and the efficient removal of NPs during the drinking water treatment process. In this study, the impact of relevant physicochemical parameters, such as pH, water hardness, and presence of natural organic matter (NOM) on the surface charge properties and aggregation abilities of both NPs and nanoplastic particles is investigated. TiO₂, CeO₂, and Polystyrene (PS) nanoplastics are selected, owing to their large number applications and contrasting characteristics at environmental pH. Experiments are performed in different water samples, including, ultrapure water, three bottled mineral waters, Lake Geneva, and drinking water produced from Lake Geneva. Our findings demonstrate that both water hardness and negatively charged natural organic matter concentrations, which were measured via dissolved organic carbon determination, are playing important roles. At environmental pH, when negatively charged nanoparticles are considered, specific cation adsorption is promoting aggregation so long as NOM concentration is limited. On the other hand, NOM adsorption is expected to be a key process in NPs destabilization when positively charged PS nanoplastics are considered.

Keywords: TiO₂ nanoparticles; CeO₂ nanoparticles; polystyrene nanoplastics; water hardness; NOM concentration; nanoparticle stability and aggregation

1. Introduction

Manufactured nanoparticles (NPs) are widely incorporated and used into a large number of consumer products and industrial applications due to their specific physicochemical properties [1,2]. Examples include the use of TiO₂ NPs in food, cosmetics [3], and photovoltaics [4], and the use of CeO₂ NPs as a fuel additives [5], in electronic devices, and cosmetics [6]. With increasing production and applications in our daily life [7], NPs are expected to diffuse in aquatic systems, through industrial discharges, wastewater treatment effluents, or surface runoff from soils [8]. Studies have shown that NPs can pose an ecotoxicological risk in aquatic environments, and possible risks to humans via, for example, their presence in water compartments, which are used for drinking water production [9,10].

Once released in the environment, the fate, mobility, and persistence of NPs in aquatic systems largely depend on their stability and possibility to form aggregates [2]. Aggregation is an important process, since aggregates containing NPs will sediment or otherwise be immobilized (via filtration process), while dispersed NPs will be able to diffuse, be more mobile, more bioavailable, and potentially more toxic. NPs stability in aquatic systems is governed by their physicochemical properties (i.e., size, coating surface charge, acid-base, and redox behavior), as well as aquatic chemical conditions, such as pH, ionic composition, and presence of natural organic matter (NOM) [11,12]. NOM is present in the majority of natural aquatic ecosystems at concentrations typically ranging from 0.1 to 10 mg/L, and is generally expected to enhance NPs stability [13–15]. Adsorbed NOM imparts a negative charge and it modifies the surface properties of NPs by raising their absolute surface potential [16,17]. Keller et al. [18] studied the behavior of three different metal oxide nanoparticles (TiO_2 , ZnO , and CeO_2) in eight different aqueous media. They showed that the adsorption of NOM onto the NPs surface significantly reduced their aggregation, stabilizing them under many environmental conditions. The presence of NOM can also induce NPs destabilization, depending on the physicochemical conditions prevailing in the medium and NOM concentration [19]. According to Wu and Cheng [15], adsorption of NOM on TiO_2 NPs is pH dependent. At low pH (< 5), NOM strongly adsorbs on positively charged TiO_2 NPs and promotes aggregation. On the other hand, high NOM concentrations can reverse the NP surface charges and promote NPs stabilization. In such conditions, divalent cations, in particular, Ca^{2+} and Mg^{2+} ions, can neutralize NP electrostatic stabilization that is enhanced by NOM and induce aggregation through cation bridging and charge neutralization mechanisms [13,17].

Studies are mainly focusing attention on the behavior and fate of metal oxide NPs in aquatic systems. However, nanoplastic particles can also represent an important source of pollution by themselves, but also via the transport, adsorption, and release of contaminants, such as heavy metals and persistent organic pollutants [20,21]. It should be noted that the environmental impact of nanoplastics differ from microplastics, because of their important surface area ratio and small size that can penetrate tissues and accumulate in organs [20,22]. Researches concerning nanoplastic particles [23] are surprisingly limited and are mainly focused on marine systems, even though fluvial systems are the main source of plastic contaminants to marine waters [24,25].

In the present work, we are studying the effect of pH, presence of NOM, and water hardness on two widespread metal oxide manufactured nanoparticles, TiO_2 and CeO_2 . Positively charged amidine Polystyrene latex particles in the nano range are also considered as nanoplastics to better understand their surface charge transformations and behavior in aquatic systems with regards to their aggregation and water chemistry. Metal oxide NPs and nanoplastic particles that were used in this study exhibit different characteristics at the pH of natural waters and consequently different chemical scenario. Indeed, at environmental pH, the surface charge of CeO_2 NPs is close to zero, whereas TiO_2 NPs exhibit negative surface charges. On the other hand, nanoplastic particles that were used in this work are positively charged in a wide range of pH and, as a result, are expected to better interact with the negatively charged NOM. The use of positively charged nanoparticles is important, since several studies have demonstrated that nanoplastic particles positively charged are more toxic to living organisms when compared to negatively charged particles [26]. First, TiO_2 , CeO_2 NPs, and nanoplastic particles are characterized in ultrapure water in a large pH domain to gain insight into their pH-responsive and aggregation behavior. Subsequently, NPs behavior in mineral, Lake Geneva, and drinking waters is evaluated by focusing on aggregation, owing to the importance of such a process in the NPs risk assessment evaluation.

2. Materials and Methods

2.1. Methods

2.1.1. Zeta Potential and Size Distribution Measurements

Determination of zeta (ζ) potential and z-average hydrodynamic diameter values of NPs in mineral, drinking, and Lake Geneva waters was achieved by laser doppler velocimetry and dynamic light scattering (DLS) methods, respectively [27]. The ζ potential was measured with a Zetasizer Nano ZS (Malvern Instruments Ltd: Malvern, UK) using the Smoluchowski approximation model and from the electrophoretic mobility determination [28]. The z-average hydrodynamic diameter was calculated from Brownian motion measurement via the Stokes-Einstein equation while using the same instrument. For each sample, five measurements of ten runs, with a delay of 5 s between them to stabilize the system, were performed to determine the ζ potential and z-average hydrodynamic diameter.

2.1.2. Scanning Electron Microscopy Imaging (SEM)

A JEOL JSM-7001FA scanning electron microscope (JEOL: Tokyo, Japan) was used to obtain images of NPs in ultrapure and Lake Geneva waters. The SEM samples were prepared by dropping 10 μ L of suspension on one aluminum stub that was covered with 5 \times 5 mm silica wafer Agar Scientific (G3390) and wrapped with platinum coating.

2.2. Materials

2.2.1. Nanoparticles

Two manufactured nanoparticles TiO₂ anatase, CeO₂ NPs, and one amidine polystyrene latex nanoplastic were used in this study. TiO₂ NPs, with a determined manufacturer x-ray diffraction diameter of 15 nm and a specific surface area of 40–60 m²/g, were purchased as a powder from Nanostructured & Amorphous Material Inc-5430MR (Los Alamos, NM, USA). The CeO₂ NPs were also purchased as a powder from Sigma-Aldrich-MKBN9764V (Buchs, Switzerland). BET determined the CeO₂ primary particle diameter < 50 nm [29], according to the manufacturer with a specific surface area of 30 m²/g. Surfactant-free polystyrene latex nanospheres with amidine functional groups on the surface were obtained from Thermo Fisher Scientific-1862725 (Rheinach, Switzerland). The aqueous dispersion contains 40 g/L of positively charged particles with a diameter that was equal to 0.09 μ m (TEM) and a specific surface area of 63 m²/g. 1 g/L stock suspensions of TiO₂ and CeO₂ NPs was prepared by diluting the previously weighted powder with ultrapure water (Milli Q water, Millipore, Switzerland, with R > 18 M Ω .cm, TOC < 2 ppb), previously adjusted to pH 3.0 \pm 0.2 to obtain a stable stock suspension. Stock suspension of TiO₂ and CeO₂ NPs were sonicated during 15 and 5 min, respectively, with an ultrasonic probe (Sonic Vibra cell, probe model CV18, Blanc Labo S.A., Switzerland) before use. Polystyrene latex nanoplastics stock suspension of 1 g/L was prepared by diluting the original suspension with ultrapure water at pH 3.0 \pm 0.2. The stock suspension of PS nanoplastics was sonicated during 15 min with a sonication bath (Bransonic ultra cleaner, Branson 5510 model, Switzerland) before use. A sonication bath was used in that case, because it was found that the ultrasonic probe promoted the aggregation of the nanoplastic particles rather than dispersion. All of the stock solutions were stored in a dark place at constant temperature of 4 °C and were used to prepare diluted suspensions for further experiments.

2.2.2. Water Samples

Five different water samples having different chemical identities, including three types of commercial bottled mineral waters (MW1, MW2, MW3), Lake Geneva, and drinking waters were selected for NPs behavior studies. The physicochemical properties of all water samples, including pH, conductivity, water hardness, and NOM concentrations as Dissolved Organic Carbon (DOC)

are given in Table 1. The choice of the three mineral waters was based on their differences in ionic composition and, in particular, water hardness. The total hardness calculation was based on Ca^{2+} and Mg^{2+} concentrations and expressed in mg CaCO_3/L . NOM was measured by considering the DOC concentrations while using a Shimadzu TOC-L instrument (Shimadzu Scientific Instruments: Kyoto, Japan). pH and conductivity were measured using a Hach Lange HQ40d portable meter (Hach Lange, Switzerland). All of the water samples were stored in a dark place and constant temperature of 4 °C.

Table 1. Bottled mineral, drinking, and Lake Geneva water properties.

Samples	pH	Conductivity (20 °C) $\pm 5 \mu\text{S}/\text{cm}$	Ionic Strength meq/L	Water Hardness $\pm 2 \text{ mg } \text{CaCO}_3/\text{L}$	DOC $\pm 0.05 \text{ mg C}/\text{L}$
Ultrapure water	adjusted	2	0	0	0.004
Mineral water 1	7.0 ± 0.1	201	2.66	63	0.28
Mineral water 2	7.2 ± 0.1	557	9.70	307	0.03
Mineral water 3	7.4 ± 0.2	2229	56.3	1474	0.25
Lake Geneva Water	8.1 ± 0.1	298	4.97	138	1.12
Drinking water	8.2 ± 0.1	310	5.04	138	0.40

2.2.3. Experimental Procedures

10 mg/L NP and nanoplastic suspensions were considered in the different water samples and they were prepared from the stock suspensions. Such a NP concentration was used in all of the experiments so as to stay in the measurement detection limit of the Zetasizer Nano. pH-titration in ultrapure water was performed for pH values in a range of 3 to 11 in order to characterize NPs and nanoplastic particles surface charge and aggregation behavior in changing pH conditions. Suspensions of NPs at $\text{pH } 3.0 \pm 0.1$ were prepared by first adding the appropriate amount of NPs from the stock suspension to obtain a final concentration of 10 mg/L and then the pH was increased. To adjust the suspension pH, small amounts of diluted hydrochloride acid and sodium hydroxide (HCl and NaOH, Titrisol® 113, Merck, Switzerland) were used. Measurements of ζ potential and z-average hydrodynamic diameters were performed every 10 min after pH modification and stabilization. For comparison of the behavior of NPs and nanoplastics in mineral, Lake Geneva, and drinking waters with a reference system, experiences in ultrapure water were first conducted by adjusting the pH to 7.0 ± 0.1 and 8.0 ± 0.1 . The aliquots of the NP stock suspension were added to the solution to obtain a final concentration of 10 mg/L. Next, experiences in mineral, Lake Geneva, and drinking waters were performed at their natural pHs. Water from Lake Geneva was filtered while using a membrane filter with pore size that was equal to 0.2 μm (Merck Millipore Ltd, Schaffhausen, Switzerland) before each experiment. The measurements of ζ potential and z-average hydrodynamic diameters were performed as a function of time during 135 min. For suspension homogenization, gentle agitation was applied during all of the experiments with a magnetic Stirrer (Lab-Mix 15, Fisher Scientific, Reinach, Switzerland) and a rotational speed equal to 100 rpm.

3. Results

3.1. Characterization of NPs and Nanoplastic Particles in Ultrapure Water

In order to evaluate the surface charge pH dependence and stability of the NPs and nanoplastic particles, the pH-titration curves in ultrapure water are determined by measuring the ζ potential and z-average hydrodynamic diameter variations as a function of pH. Figure 1a presents the results for TiO_2 NPs. The surface of TiO_2 NPs is found to be strongly positively charged at pH 3.0 ($+31 \pm 0.5 \text{ mV}$).

By further increasing the pH, the ζ potential decreases until the point of zero charge (PZC) at $\text{pH}_{\text{pzc}} = 5.8 \pm 0.1$. This value is close to the experimental value of $\text{pH}_{\text{pzc}} = 6.2$ that was obtained by Loosli et al. [30]. When the pH is higher than pH_{pzc} , the surface charge becomes negative and stable at $-40 \pm 2 \text{ mV}$ at pH 10 ± 0.1 . The z-average hydrodynamic diameter of TiO_2 NPs is found stable below pH 5.0 with values that are equal to $430 \pm 10 \text{ nm}$. Subsequently, fast aggregation is observed

with a maximum value of 887 ± 40 nm in the PZC region. A further pH increase leads to the decrease of the TiO_2 hydrodynamic diameter, indicating reversible aggregation. When $\text{pH} \geq 8.0$, TiO_2 NPs exhibit a stable domain with values of z-average hydrodynamic diameter equal to 405 ± 10 nm in good agreement with the SEM image of TiO_2 , as presented in Figure 1b. TiO_2 NPs destabilization is observed in a ζ potential range between +20 and −25 mV, as indicated in the gray area (Figure 1a).

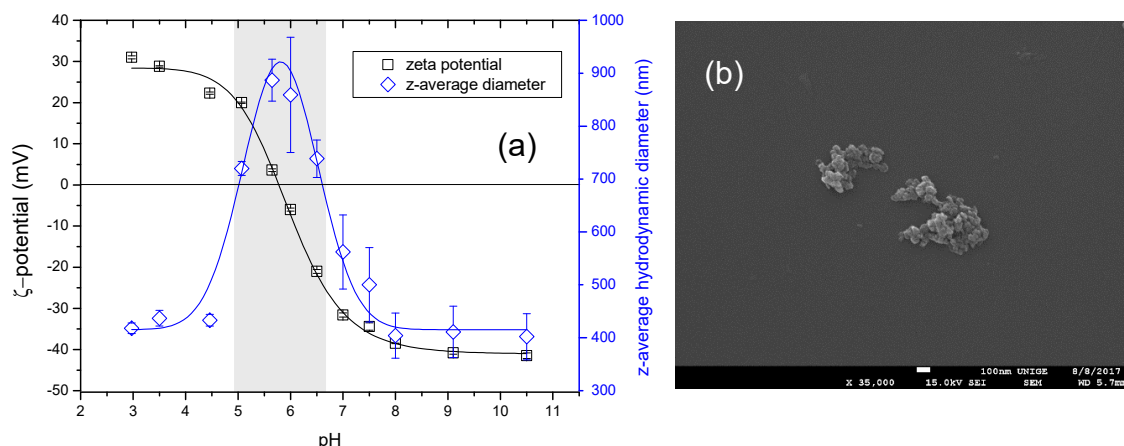


Figure 1. (a) Zeta (ζ) potential and z-average hydrodynamic diameter variation of TiO_2 nanoparticles (NPs) (10 mg/L) as a function of pH in ultrapure water. The point of zero charge (PZC) is found at $\text{pH}_{\text{PZC}} = 5.8 \pm 0.1$. Aggregation is observed in the PZC region (gray domain) (b). SEM image of TiO_2 NPs in ultrapure water at $\text{pH} > \text{pH}_{\text{PZC}}$. Aggregates diameters are found consistent with dynamic light scattering (DLS) analysis. Lines connecting data are given to guide the eye.

As shown in Figure 2a, CeO_2 NPs exhibit a stable and positive charge ($+21 \pm 1$ mV) from pH 3.0 to 5.0. Subsequently, ζ potential rapidly decreases to reach the PZC at $\text{pH}_{\text{PZC}} = 6.9 \pm 0.1$, which is similar to the previously reported studies [31]. An increase of pH leads to charge reversal with ζ potential values equals to -32 ± 2 mV at $\text{pH} 10 \pm 0.1$. As illustrated in Figure 2a, the z-average diameter of CeO_2 NPs is stable below pH 6.0 with values that are equal to 350 ± 50 nm. Near the PZC region z-average diameter increases until values that are greater than $1.5 \mu\text{m}$, a further pH increase leads to charge reversal. However, CeO_2 aggregates are found to be stable and are not affected by pH increase, as observed for TiO_2 , since no significant decrease of the z-average diameter is observed after the PZC, which is also confirmed by SEM (Figure 2b).

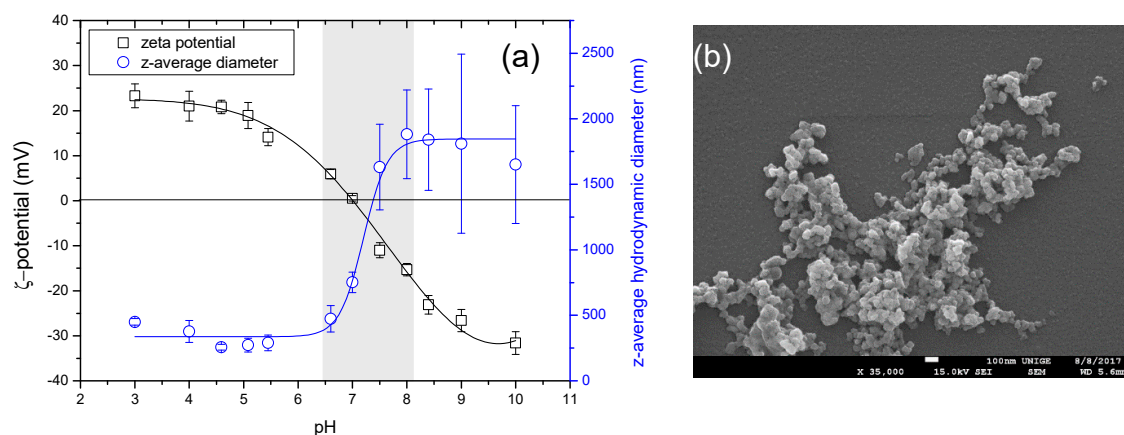


Figure 2. (a) ζ potential and z-average hydrodynamic diameter variation of CeO_2 NPs (10 mg/L) as a function of pH in ultrapure water. The point of zero charge (PZC) is found equal to $\text{pH}_{\text{PZC}} = 6.9 \pm 0.1$. Strong aggregation is observed around the PZC region (gray domain) in agreement with SEM image (b) SEM image of CeO_2 NPs aggregates in ultrapure water at $\text{pH} > \text{pH}_{\text{PZC}}$.

The surface charge and stability domain of polystyrene latex nanoplastics versus pH are illustrated in Figure 3a. PS nanoplastics are found to be strongly positively charged and stable at $\text{pH} < 7.0$ with values that are equal to $+50 \pm 1$ mV. By increasing pH, surface charge of nanoplastics decrease to the PZC at $\text{pH}_{\text{PZC}} = 9.9 \pm 0.1$ as (Figure 3a), which is close to the value that was obtained by Cross et al. [32] with $\text{pH}_{\text{PZC}} = 9.5$. Subsequently, charge reversal occurs by further increasing the pH. No aggregation is observed below pH 9.0 and nanoplastics remain stable with a z-average diameter that is equal to 98 ± 2 nm. Such a pH-surface charge behavior is related to the high pKa value of amidine functional group, which is approximately equal to 12 [33]. Aggregation is observed in the PZC region with a maximum z-average diameter value of 1260 ± 190 nm. SEM picture (Figure 3b) indicates that the PS nanoplastics are spherical and highly monodispersed.

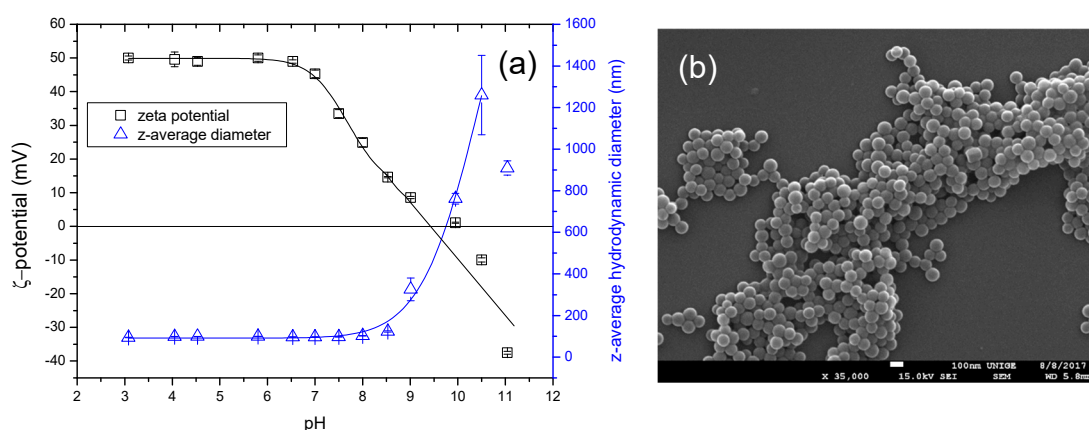


Figure 3. (a) ζ potential and z-average hydrodynamic diameter variation of amidine PS nanoplastic particles (10 mg/L) as a function of pH in ultrapure water. The point of zero charge (PZC) is found at $\text{pH} = 9.9 \pm 0.1$. Aggregation is observed around the PZC region (gray domain), and (b) SEM image of PS nanoplastic aggregates in ultrapure water at $\text{pH} > \text{pH}_{\text{PZC}}$. SEM analysis indicates spherical and monodispersed nanoplastics.

3.2. Behavior of NPs and Nanoplastic Particles in Mineral, Lake Geneva and Drinking Waters

To understand the impact of the physicochemical properties of mineral, drinking, and Lake Geneva waters, such as water hardness and dissolved organic matter concentration on NPs and nanoplastics stability, time-resolved measurements were made to provide information on particle surface charge and z-average diameter variations. Experiments with 10 mg/L NPs and nanoplastic suspensions in five different water samples (Table 1) were conducted to evaluate their stability with time. Ultrapure water was used as a reference system to better explain the changes with time, effects of water hardness, organic matter, and ionic strength in the different waters.

3.2.1. TiO_2 Nanoparticles

The stability of TiO_2 NPs in bottled mineral waters as a function of time is first considered. The ζ potential and z-average hydrodynamic diameter of TiO_2 NPs in MW1, MW2, and MW3 are presented for comparison in Figure 4a. In ultrapure water that was adjusted at the pH of the mineral waters i.e., $\text{pH} 7.0 \pm 0.1$, ζ potential and z-average hydrodynamic diameters are found to be stable with time. TiO_2 NPs are negatively charged with a ζ potential value equal to -28 ± 3 mV and z-average hydrodynamic diameter in the range of 466 ± 4 nm. The reason of such stability is due to the presence of repulsive forces between negatively charged TiO_2 particles.

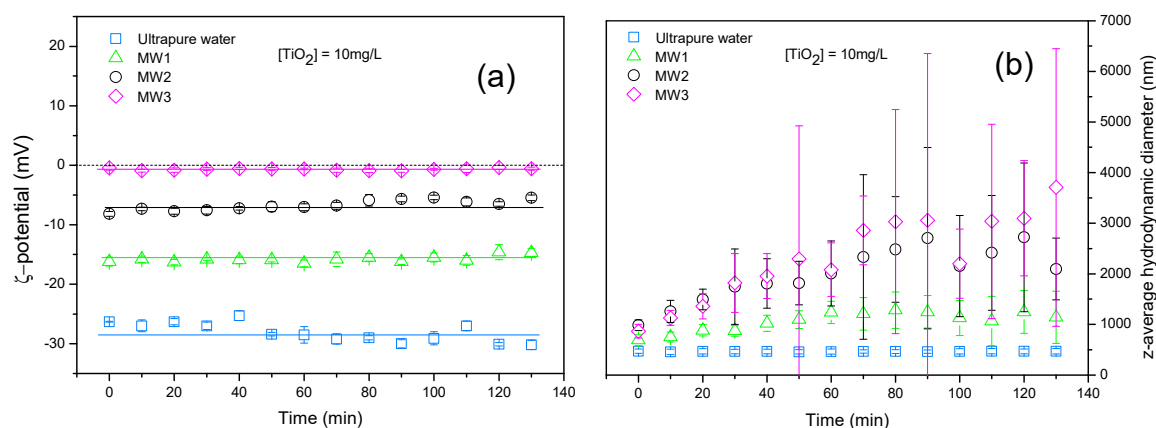


Figure 4. (a) ζ potential and (b) z-average hydrodynamic diameter variation of TiO_2 as a function of time in ultrapure water at $\text{pH} = 7.0 \pm 0.1$ and mineral waters at their natural pHs. TiO_2 surface charge is found to be reduced and neutralized in mineral waters hence resulting in TiO_2 aggregation.

By considering MWs, a systematic decrease in ζ potential, i.e., less negative values, is observed, which is found to be proportional to the mineral water hardness. The presence of divalent ions, such as Ca^{2+} and Mg^{2+} , is found here to strongly modify the stability of negatively charged TiO_2 NPs via specific adsorption. As shown in Figure 4a, at a low concentration of divalent ions (MW1), TiO_2 NPs are found to be less stable than in ultrapure water, which is in good agreement with their surface charge (-16 ± 1 mV). As a result, a continuous increase of aggregate size is observed within the experimental time (135 min), with a maximum value equal to 1200 ± 26 nm. Aggregation is more pronounced when TiO_2 NPs are added into MW3. As the water hardness increases (from MW1 to MW3), surface charge is more effectively neutralized due to both the specific adsorption and surface charge screening effect, resulting in the formation of larger TiO_2 aggregates with z-average hydrodynamic diameters of up to $2.5 \mu\text{m}$.

Regarding the stability of TiO_2 NPs in Lake Geneva and drinking water (Figure 5a), a significant decrease in ζ potential is also observed with values equal to -13 ± 1 mV and -8 ± 1 mV, respectively. These values are close to the zeta potential measurements that were made by Loosli et al. [30] and Graham et al. [34] for TiO_2 NPs and natural colloids from the Geneva Lake. Lake Geneva water contains multivalent cations (Ca^{2+} and Mg^{2+}), but also natural organic matter. As natural organic matter is negatively charged, the Ca^{2+} ions are expected to promote the adsorption of NOM and act as bridges between the NOM and the TiO_2 NPs surface [12,13,35]. As shown in Figure 5b, TiO_2 NPs are stable with time in ultrapure water with z-average diameters that are equal to 460 ± 12 nm. NPs are found to be unstable in surface waters, especially in drinking waters where aggregates are rapidly formed with sizes that are greater than 2000 nm after 60 min. On the other hand, aggregation is less important for NPs in Lake Geneva water with z-average diameters equal to 1550 ± 23 nm after 135 min. This can be mainly explained by the higher DOC concentration in Lake Geneva water when compared to drinking water, as indicated in Table 1. In such conditions, NOM is expected to reduce the impact of Ca^{2+} and Mg^{2+} ions on the final TiO_2 surface charge, as shown by Loosli et al. [30]

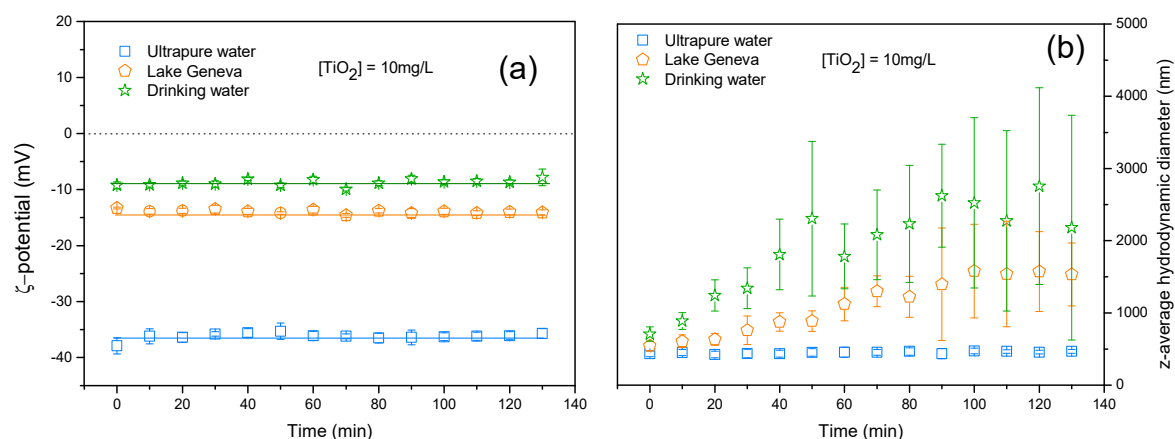


Figure 5. (a) ζ potential and (b) z-average hydrodynamic diameter variation of TiO₂ as a function of time in ultrapure water at pH = 8.0 ± 0.1 , drinking, and Lake Geneva waters at their natural pHs. In comparison to ultrapure water, ζ potential decreases towards less negative values when TiO₂ NPs are introduced in drinking and Lake Geneva water, hence promoting aggregation.

3.2.2. CeO₂ Nanoparticles

In Figure 6a, are presented the ζ potential and z-average hydrodynamic diameter variation of CeO₂ NPs in mineral waters as a function of time. The surface charge of CeO₂ NPs in ultrapure water is negative with a ζ potential value that is equal to -7 ± 1 mV. As expected, a decrease in ζ potential value is observed in MWs, which can also be related to water hardness. Indeed, when NPs are added to MW2 and MW3, charge inversion is achieved and surface charge is found to be slightly positive with ζ potential values equal to $+2.5 \pm 1$ mV and $+5 \pm 1$ mV, respectively. Such a behavior indicates strong affinity between the divalent cation and CeO₂ negative surface. Aggregation is observed for all water samples with z-average hydrodynamic diameters greater than 1 μm within the experimental time (Figure 6b). The highly variable CeO₂ diameters in ultrapure water range from 500 nm to 3000 nm, which is the result of a ζ potential close to zero (-8 mV), and is thus situated in the PZC region.

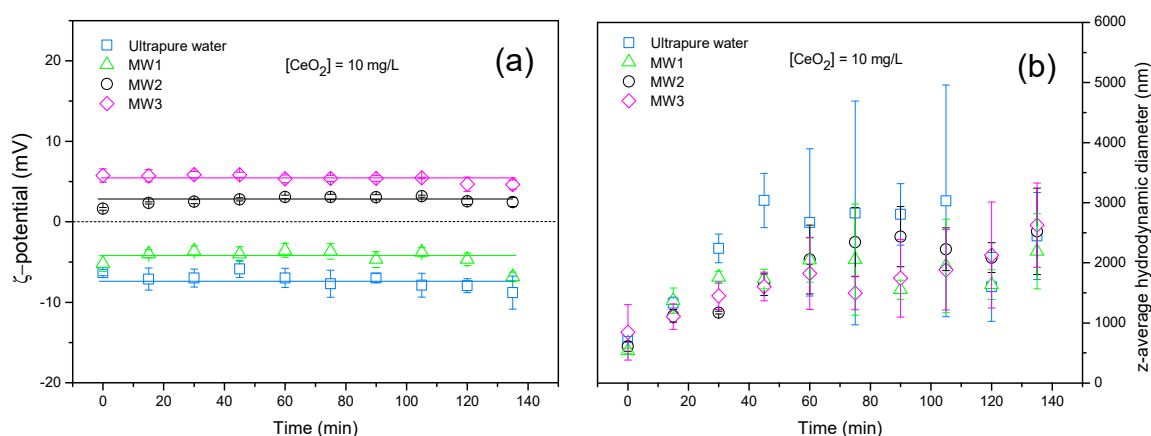


Figure 6. (a) ζ potential and (b) z-average hydrodynamic diameter variation of CeO₂ as a function of time in ultrapure water at pH = 7.0 ± 0.1 and mineral waters at their natural pHs. CeO₂ NPs surface charge is found to be reduced in all mineral waters, hence promoting CeO₂ aggregation.

The results for CeO₂ NPs stability in Lake Geneva and drinking waters are presented in Figure 7. A decrease in ζ potential is observed in both waters with values that are equal to -11 ± 1 mV and -6 ± 1 mV, respectively. CeO₂ NPs are aggregated in all water samples, as shown in Figure 7b.

As discussed for TiO₂ NPs, the adsorption of divalent cations are also expected here to interact with CeO₂ NPs and NOM, forming bridges between them, resulting in NPs destabilization. As

shown for drinking water, 0.4 mg/L DOC lead to CeO_2 NPs aggregation with z-average diameters that are greater than 2 μm . However, limited aggregation is observed for NPs in Lake Geneva water with z-average diameters of less than 1 μm due to the presence of DOC at significant concentrations (1.12 mg/L), enhancing NPs stability. Our results are in agreement with those that were obtained by Oriekhova and Stoll [31]. The authors found CeO_2 NPs aggregated in Lake Geneva water with time and negative surface charge with a zeta potential equal to -13.3 ± 0.6 mV.

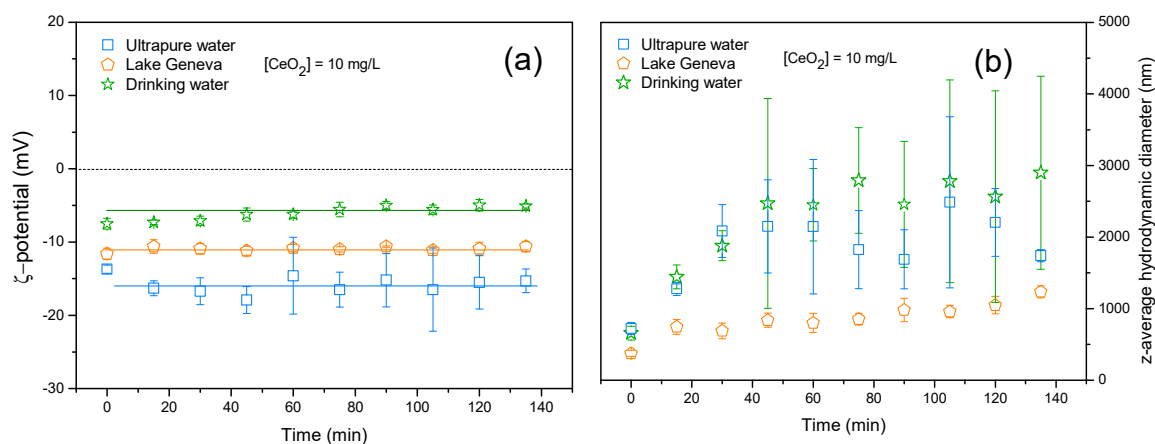


Figure 7. (a) ζ potential and (b) z-average hydrodynamic diameter variation of CeO_2 as a function of time in ultrapure water at $\text{pH} = 8.0 \pm 0.1$, drinking and Lake Geneva waters at their natural pHs. Limited aggregation is observed due to the presence of DOC at a significant concentration (1.12 mg/L) when CeO_2 NPs are introduced in Lake Geneva water.

3.2.3. Polystyrene Nanoplastic Particles

Nanoplastics behavior in mineral waters is presented in Figure 8 and a comparison is made with ultrapure water. In ultrapure water, the surface charge is found to be stable and PS nanoplastics are strongly positively charged ($+41 \pm 3$ mV), with z-average hydrodynamic diameter values that are equal to 98 ± 3 nm. When nanoplastics are added in mineral waters, a decrease of ζ potential is observed because of the presence of small amounts of negatively charged DOC (Table 1). Despite the decrease of ζ potential, nanoplastics are stable in almost all cases and no aggregation is observed due to the positive amidine functional groups, making nanoplastics resistant in MW1 and MW2 to aggregation effects of divalent ions and the presence of NOM.

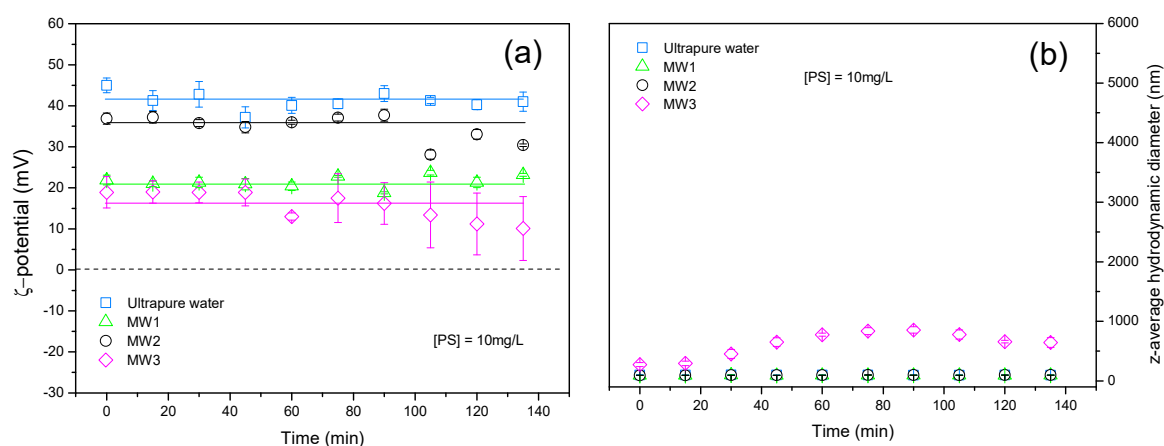


Figure 8. (a) ζ potential and (b) z-average hydrodynamic diameter variation of amidine PS nanoplastic particles as a function of time in ultrapure at $\text{pH} = 7.0 \pm 0.1$ and mineral waters at their natural pHs. A decrease of ζ potential is observed for all mineral waters. However, nanoplastics are stable and no aggregation is observed. Limited aggregation is only observed for MW3.

As shown in Figure 8b, limited aggregation is only observed for MW3, which is in agreement with the corresponding ζ potential values, which are found less than +20 mV. On the other hand, when nanoplastic particles are added in Lake Geneva and drinking water, a significant decrease of ζ potential is observed. As can be seen in Figure 9a, the surface charge of nanoplastics in drinking water significantly decreases but remains positive at about +10 mV, resulting in aggregation, as indicated in Figure 9b.

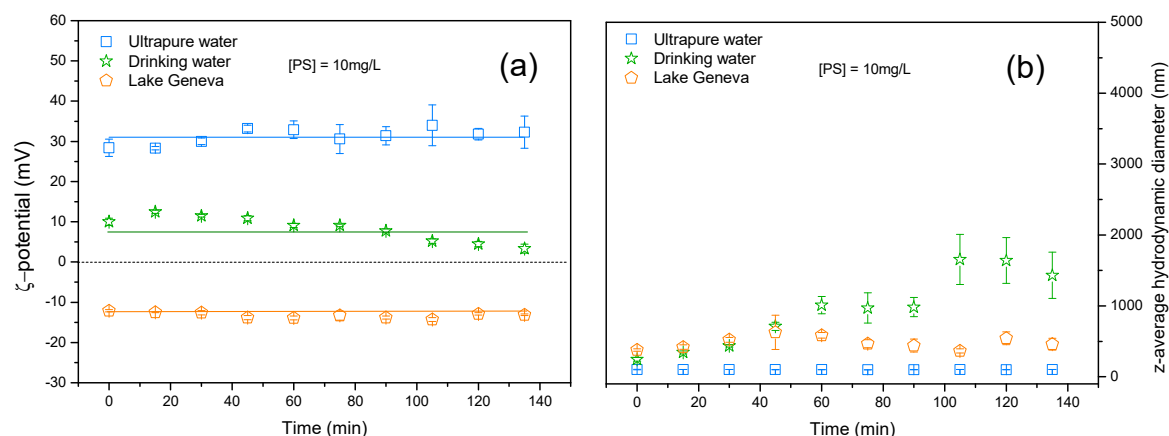


Figure 9. (a) ζ potential and (b) z-average hydrodynamic diameter variation of amidine PS nanoplastic particles as a function of time in ultrapure at $\text{pH} = 8.0 \pm 0.1$, drinking and Lake Geneva waters at their natural pHs. Charge reversal is observed when PS nanoplastic particles are introduced in Lake Geneva water. Natural organic matter (NOM) coating is expected and results in limited aggregation of nanoplastics.

In Lake Geneva water, high concentrations of NOM lead to charge reversal (-13 ± 1 mV), and nanoplastics remain relatively stable with a z-average hydrodynamic diameter of 450 ± 100 nm. This indicates that NOM coating in Lake Geneva is reducing nanoplastic aggregation due to steric stabilization effects. NOM coating is illustrated from a morphological point of view in the SEM image that is presented in Figure 10. PS nanoplastic shapes are no more spherical, but slightly ellipsoidal and fuzzy membranes surrounding the particles are producing less contrasted images.

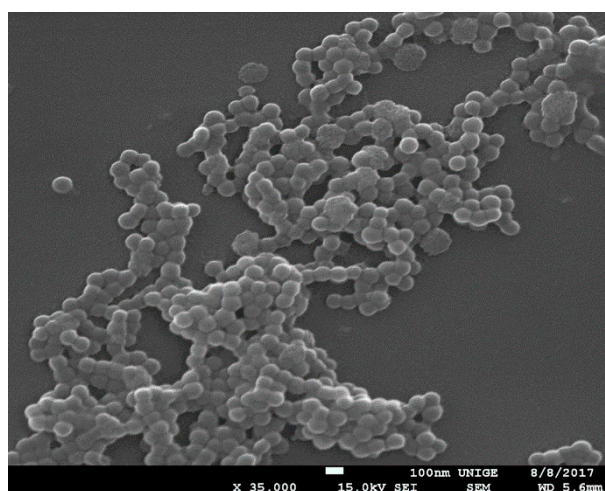


Figure 10. Scanning Electron Microscopy (SEM) image of amidine PS nanoplastic particles (10 mg/L) in filtered ($0.2 \mu\text{m}$) Lake Geneva water at $\text{pH} 8.1 \pm 0.1 < \text{pH}_{\text{pzc}}$. When compared to ultrapure water (Figure 3b) where, $\text{pH} > \text{pH}_{\text{pzc}}$. PS nanoplastic aggregates are found coated with a complex organic matter matrix resulting in a fuzzy particle contrast.

3.2.4. Impact of Water Hardness and Organic Matter

To better highlight the influence of both water hardness and NOM on the aggregation behavior of NPs and nanoplastics, stability diagrams were calculated from the z-average hydrodynamic diameter values that were obtained in the different conditions, and they are presented in Figure 11 for TiO₂ and CeO₂ NPs, and nanoplastics. All of the results dealing with aggregate formation obtained in MWs, drinking and Lake Geneva waters have merged together. Red color indicates that NPs are dispersed, whereas blue color indicates strong aggregation i.e., the formation of aggregates with sizes that are greater than 2000 nm. For TiO₂ NPs, aggregation is found to be promoted by increasing water hardness so long as the DOC concentration is less than 0.6 mg/L. This indicates that divalent ions, such as Ca²⁺ and Mg²⁺, are effective in neutralizing TiO₂ NPs negative surface charge. As TiO₂ NPs are strongly negatively charged at environmental pH, Ca²⁺ and Mg²⁺ are strongly adsorbed onto TiO₂ due to the attractive electrostatic forces between NPs and divalent cations, resulting in TiO₂ NPs charge neutralization. Increasing DOC concentration is found to reduce the aggregation of TiO₂ NPs, which is probably due to the formation of Ca²⁺ and Mg²⁺ complexes reducing the impact of these ions on the TiO₂ surface charge. On the other hand, water hardness is found to have a less significant role on CeO₂ NPs aggregation. At environmental pH, the surface charge of CeO₂ NPs is close to the PZC (pH_{PZC} = 6.9 ± 0.1) and, consequently, in most conditions, NPs are already aggregated. The stability of CeO₂ NPs with regards to water hardness is caused by the repulsive forces between NPs and divalent ions (Ca²⁺ and Mg²⁺). DOC increase (above 0.8 mg/L) is also found to reduce aggregation. On the other hand, polystyrene nanoplastics, which are strongly positively charged at environmental pH, are found to be more stable with regards to water hardness and natural organic matter. PS nanoplastics are stabilized against water hardness due to electrostatic repulsive interaction between the amidine functional group and ions Ca²⁺ and Mg²⁺. Negatively charged NOM can adsorb onto positively charged NPs promoting aggregation by charge neutralization and via bridging mechanisms that are induced by the presence of divalent cations [33]. However, PS nanoplastics aggregation is observed in a limited domain with specific water hardness and DOC. This is an important issue, indicating that, in general, the polystyrene nanoplastics stability and dispersion state are more pronounced in aquatic systems.

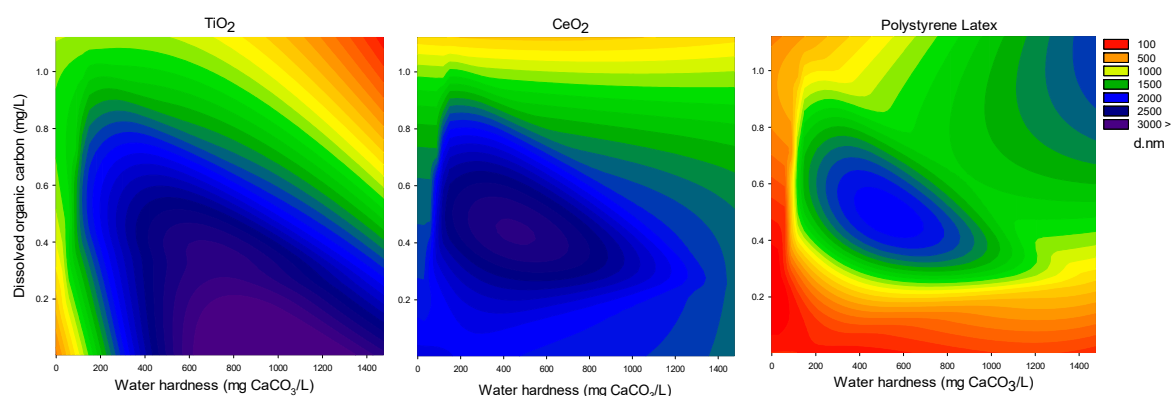


Figure 11. Aggregation intensity diagrams of TiO₂, CeO₂, and amidine PS nanoplastic particles as a function of water hardness and Dissolved Organic Carbon (DOC) in MW and SW at a 10 mg/L TiO₂, CeO₂ and PS nanoplastic concentration. The color and respective values in the legend represent the z-average diameter of NPs and PS nanoplastic particles in nanometers that were obtained after 1h. Blue color indicates significant aggregation, whereas red color indicates limited aggregation.

4. Conclusions

In this study, the importance of several relevant environmental parameters on the stability of NPs and PS nanoplastics in various waters was evaluated. In ultrapure water, TiO₂ and PS nanoplastic were found stable, while CeO₂ NPs was found to aggregate with time. In bottled mineral waters, TiO₂

and CeO₂ NPs were found to be aggregated. The presence of divalent ions, such as Ca²⁺ and Mg²⁺, induced the aggregation of negatively charged NPs by adsorption and charge neutralization, hence reducing electrostatic forces. In contrast, positively charged PS nanoplastics, were found to remain stable against aggregation. In surface waters, such as drinking and Lake Geneva waters, NPs, as well as nanoplastic particles, were systematically destabilized, especially in drinking water with low NOM concentration when compared with Lake Geneva water. This indicates that high NOM concentrations, such as in Lake Geneva, is limiting NPs and PS nanoplastic aggregation due to steric stabilization effects. Although nanoplastic particles were destabilized in specific conditions, such positive particles have longer residence times and form small aggregates that will be difficult to eliminate via filtration processes. Our research indicates that fate and transport of nanoparticles, including nanoplastics, in aquatic systems are strongly governed by their surface properties and physicochemical conditions of the medium (water hardness, pH, NOM concentration). Future research will focus on coagulation processes that provide an effective way for NPs removal during water treatment.

Author Contributions: Methodology, L.R.; Software, L.R.; Validation, S.S., S.R.G. and S.Z.; Writing—original draft preparation, L.R.; Writing—review and editing, S.S., S.R.G. and S.Z.; Supervision, S.S.

Funding: This research was funded by FOWA from Société Suisse de l'Industrie du Gaz et des Eaux SSIGE/SGW.

Acknowledgments: The authors acknowledge support received from FOWA fund from Société Suisse de l'Industrie du Gaz et des Eaux SSIGE/SGW, Service Industriel de Genève (SIG) and University of Geneva. We are also grateful to Agathe Martignier for her support during the SEM measurements.

Conflicts of Interest: The authors declare no conflict of interest.

References

1. Auffan, M.; Rose, J.; Bottero, J.-Y.; Lowry, G.V.; Jolivet, J.-P.; Wiesner, M.R. Towards a definition of inorganic nanoparticles from an environmental, health and safety perspective. *Nat. Nanotechnol.* **2009**, *4*, 634–641. [[CrossRef](#)]
2. Troester, M.; Brauch, H.-J.; Hofmann, T. Vulnerability of drinking water supplies to engineered nanoparticles. *Water Res.* **2016**, *96*, 255–279. [[CrossRef](#)]
3. Weir, A.; Westerhoff, P.; Fabricius, L.; Hristovski, K.; von Goetz, N. Titanium dioxide nanoparticles in food and personal care products. *Environ. Sci. Technol.* **2012**, *46*, 2242–2250. [[CrossRef](#)] [[PubMed](#)]
4. Chen, X.; Mao, S.S. Titanium dioxide nanomaterials: Synthesis, properties, modifications, and applications. *Chem. Rev.* **2007**, *107*, 2891–2959. [[CrossRef](#)] [[PubMed](#)]
5. Cassee, F.R.; van Balen, E.C.; Singh, C.; Green, D.; Muijsers, H.; Weinstein, J.; Dreher, K. Exposure, health and ecological effects review of engineered nanoscale cerium and cerium oxide associated with its use as a fuel additive. *Crit. Rev. Toxicol.* **2011**, *41*, 213–229. [[CrossRef](#)]
6. Grinter, D.C.; Muryn, C.; Sala, A.; Yim, C.-M.; Pang, C.L.; Mentes, T.O.; Locatelli, A.; Thornton, G. Spillover reoxidation of ceria nanoparticles. *J. Phys. Chem. C* **2016**, *120*, 11037–11044. [[CrossRef](#)]
7. Khan, W.S.; Asmatulu, R. Chapter 1—Nanotechnology emerging trends, markets, and concerns. In *Nanotechnology Safety*; Elsevier: Amsterdam, The Netherlands, 2013; pp. 1–16.
8. Batley, G.E.; Kirby, J.K.; McLaughlin, M.J. Fate and risks of nanomaterials in aquatic and terrestrial environments. *Acc. Chem. Res.* **2013**, *46*, 854–862. [[CrossRef](#)]
9. Bhatt, I.; Tripathi, B.N. Interaction of engineered nanoparticles with various components of the environment and possible strategies for their risk assessment. *Chemosphere* **2011**, *82*, 308–317. [[CrossRef](#)] [[PubMed](#)]
10. Park, C.M.; Chu, K.H.; Her, N.; Jang, M.; Baalousha, M.; Heo, J.; Yoon, Y. Occurrence and removal of engineered nanoparticles in drinking water treatment and wastewater treatment processes. *Sep. Purif. Rev.* **2017**, *46*, 255–272. [[CrossRef](#)]
11. Zhang, Y.; Chen, Y.; Westerhoff, P.; Hristovski, K.; Crittenden, J.C. Stability of commercial metal oxide nanoparticles in water. *Water Res.* **2008**, *42*, 2204–2212. [[CrossRef](#)] [[PubMed](#)]

12. French, R.A.; Jacobson, A.R.; Kim, B.; Isley, S.L.; Penn, R.L.; Baveye, P.C. Influence of ionic strength, pH, and cation valence on aggregation kinetics of titanium dioxide nanoparticles. *Environ. Sci. Technol.* **2009**, *43*, 1354–1359. [[CrossRef](#)] [[PubMed](#)]
13. Philippe, A.; Schaumann, G.E. Interactions of dissolved organic matter with natural and engineered inorganic colloids: A review. *Environ. Sci. Technol.* **2014**, *48*, 8946–8962. [[CrossRef](#)] [[PubMed](#)]
14. Baalousha, M.; Nur, Y.; Römer, I.; Tejamaya, M.; Lead, J.R. Effect of monovalent and divalent cations, anions and fulvic acid on aggregation of citrate-coated silver nanoparticles. *Sci. Total Environ.* **2013**, *454*–*455*, 119–131. [[CrossRef](#)]
15. Wu, Y.; Cheng, T. Stability of nTiO₂ particles and their attachment to sand: Effects of humic acid at different pH. *Sci. Total Environ.* **2016**, *541*, 579–589. [[CrossRef](#)]
16. Serrão Sousa, V.; Corniciuc, C.; Ribau Teixeira, M. The effect of TiO₂ nanoparticles removal on drinking water quality produced by conventional treatment C/F/S. *Water Res.* **2017**, *109*, 1–12. [[CrossRef](#)]
17. Zhang, Y.; Chen, Y.; Westerhoff, P.; Crittenden, J. Impact of natural organic matter and divalent cations on the stability of aqueous nanoparticles. *Water Res.* **2009**, *43*, 4249–4257. [[CrossRef](#)] [[PubMed](#)]
18. Keller, A.A.; Wang, H.; Zhou, D.; Lenihan, H.S.; Cherr, G.; Cardinale, B.J.; Miller, R.; Ji, Z. Stability and aggregation of metal oxide nanoparticles in natural aqueous matrices. *Environ. Sci. Technol.* **2010**, *44*, 1962–1967. [[CrossRef](#)]
19. Loosli, F.; Le Coustumer, P.; Stoll, S. Effect of natural organic matter on the disagglomeration of manufactured TiO₂ nanoparticles. *Environ. Sci. Nano* **2014**, *1*, 154–160. [[CrossRef](#)]
20. Lambert, S.; Wagner, M. Characterisation of nanoplastics during the degradation of polystyrene. *Chemosphere* **2016**, *145*, 265–268. [[CrossRef](#)]
21. Alimi, O.S.; Farner Budarz, J.; Hernandez, L.M.; Tufenkji, N. Microplastics and nanoplastics in aquatic environments: Aggregation, deposition, and enhanced contaminant transport. *Environ. Sci. Technol.* **2018**, *52*, 1704–1724. [[CrossRef](#)]
22. Mattsson, K.; Hansson, L.A.; Cedervall, T. Nano-plastics in the aquatic environment. *Environ. Sci. Process. Impacts* **2015**, *17*, 1712–1721. [[CrossRef](#)] [[PubMed](#)]
23. Oriekhova, O.; Stoll, S. Heteroaggregation of nanoplastic particles in the presence of inorganic colloids and natural organic matter. *Environ. Sci. Nano* **2018**, *5*, 792–799. [[CrossRef](#)]
24. Eerkes-Medrano, D.; Thompson, R.C.; Aldridge, D.C. Microplastics in freshwater systems: A review of the emerging threats, identification of knowledge gaps and prioritisation of research needs. *Water Res.* **2015**, *75*, 63–82. [[CrossRef](#)] [[PubMed](#)]
25. Ter Halle, A.; Jeanneau, L.; Martignac, M.; Jardé, E.; Pedrono, B.; Brach, L.; Gigault, J. Nanoplastic in the north Atlantic subtropical gyre. *Environ. Sci. Technol.* **2017**, *51*, 13689–13697. [[CrossRef](#)] [[PubMed](#)]
26. Bergami, E.; Pugnali, S.; Vannuccini, M.L.; Manfra, L.; Faleri, C.; Savorelli, F.; Dawson, K.A.; Corsi, I. Long-term toxicity of surface-charged polystyrene nanoplastics to marine planktonic species *Dunaliella tertiolecta* and *Artemia franciscana*. *Aquat. Toxicol.* **2017**, *189*, 159–169. [[CrossRef](#)] [[PubMed](#)]
27. Gregory, J. *Particles in Water: Properties and Processes*; CRC Press: Boca Raton, FL, USA, 2005.
28. Lowry, G.V.; Hill, R.J.; Harper, S.; Rawle, A.F.; Hendren, C.O.; Klaessig, F.; Nobbmann, U.; Sayre, P.; Rumble, J. Guidance to improve the scientific value of zeta-potential measurements in nanoEHS. *Environ. Sci. Nano* **2016**, *3*, 953–965. [[CrossRef](#)]
29. Bruanuer, S.; Emmett, P.H.; Teller, E. Adsorption of gases in multimolecular layers. *J. Am. Chem. Soc.* **1938**, *60*, 309–316. [[CrossRef](#)]
30. Loosli, F.; Le Coustumer, P.; Stoll, S. Effect of electrolyte valency, alginate concentration and pH on engineered TiO₂ nanoparticle stability in aqueous solution. *Sci. Total Environ.* **2015**, *535*, 28–34. [[CrossRef](#)] [[PubMed](#)]
31. Oriekhova, O.; Stoll, S. Stability of uncoated and fulvic acids coated manufactured CeO₂ nanoparticles in various conditions: From ultrapure to natural Lake Geneva waters. *Sci. Total Environ.* **2016**, *562*, 327–334. [[CrossRef](#)] [[PubMed](#)]
32. Cross, W.M.; Ma, S.; Winter, R.M.; Kellar, J.J. FT-IR/ATR and SEM study of colloidal particle deposition. *Colloids Surf. A Physicochem. Eng. Asp.* **1999**, *154*, 115–125. [[CrossRef](#)]
33. Oszczapowicz, J.; Raczynska, E. Amidines. Part 13. Influence of substitution at imino nitrogen atom on pK_a values of N¹N¹-Dimethylacetamidines. *J. Chem. Soc. Perkin Trans. 2* **1984**, *10*, 1643–1646. [[CrossRef](#)]

34. Graham, N.D.; Stoll, S.; Loizeau, J.-L. Colloid characterization at the sediment-water interface of Vidy Bay, Lake Geneva. *Fundam. Appl. Limnol.* **2014**, *184*, 87–100. [[CrossRef](#)]
35. Erhayem, M.; Sohn, M. Stability studies for titanium dioxide nanoparticles upon adsorption of Suwannee River humic and fulvic acids and natural organic matter. *Sci. Total Environ.* **2014**, *468–469*, 249–257. [[CrossRef](#)] [[PubMed](#)]



© 2019 by the authors. Licensee MDPI, Basel, Switzerland. This article is an open access article distributed under the terms and conditions of the Creative Commons Attribution (CC BY) license (<http://creativecommons.org/licenses/by/4.0/>).